THEORETICA CHIMICA ACTA

Theoret. Chim. Acta (Berl.) 62, 55–67 (1982)

© Springer -Verlag 1982

Binding/Antibinding Analyses for Diatomic Interactions. The Effect of Nuclear Charge on One-Electron Chemical Bonding

Toshikatsu Koga, Akihiro Hirashima, Yuji Ueda, and Mutsuo Morita

Department of Applied Chemistry and Department of Applied Science for Energy, Muroran Institute of Technology, Muroran, Hokkaido, 050 Japan

For a one-electron homonuclear diatomic system with arbitrary nuclear charge Z, the change in the nature of diatomic interaction and its density origin are quantitatively examined as a function of Z by the method of binding/antibinding analyses based on the Hellmann–Feynman theorem. In the $1s\sigma_g$ ground state, two energy extrema, potential barrier at a large internuclear distance and potential minimum at a smaller distance, appear for $1 < Z < 1.44$. The binding part of the partitioned Hellmann–Feynman forces suffers little effect of Z, and these two extrema are attributed respectively to the increase in the nuclear repulsion and to the decrease in the antibinding part of the partitioned forces. In the "antibonding" $2p\sigma_u$ state, a stable molecule is formed for $Z < 1$. This appearance of the bonding nature is shown to have its origin in the binding part which is almost unchanged by the decrease of Z.

Key words: Nuclear charge effect – Chemical bonding – Hellmann–Feynman theorem.

1. Introduction

The distribution of diatomic electron density is regionally separated into binding and antibinding parts by the Berlin diagram [1, 2] based on the Hellmann–Feynman theorem [3]. This partitioning provides a unique interpretation for the role of the electron density in chemical bonding from the viewpoint of quantum-mechanical force. Namely, the binding density gives binding force which works to pull the two nuclei together, while the antibinding density gives

0040-5744/82/0062/0055/$02.60

antibinding force which works to push them apart in cooperation with the nuclear repulsion. The simplicity and visuality of the Berlin diagram have been qualitatively but successfully used to interpret and predict the dynamic behaviour of the electron density in various nuclear rearrangement processes [4, 5].

Recently, we have given quantitative examinations of such regional partitioning of electron density for several one-electron diatomic systems [6–8]. Based on the exact wave functions, the electronic charge, interatomic force, and stabilization energy have been divided into the binding and antibinding parts and their contributions during the attractive/repulsive and σ/π interaction processes have been analyzed in detail. Introducing the center of electron density (CED) as a measure, we have also clarified the dynamic behaviour of the electron density. In the study of the HeH^{2+} system [7], the effect of the increased nuclear charge on the density reorganization and the resultant interatomic force of the system have been discussed in comparison with the H_2^+ system [6]. From the force-theoretical point of view, it has been suggested whether the relevant electron density is loosely or tightly bound to the nuclei is important in characterizing the bonding.

The purpose of this paper is to examine systematically the effect of nuclear charge on the nature of chemical bonding by monitoring the behaviour of interatomic force and its density origin. We have again chosen the one-electron homonuclear diatomic system with an arbitrary nuclear charge Z, since we know the exact wave function for this system. Then, we can rigorously apply the method of binding/antibinding analyses [6–8] and the results are exactly reliable within the fixed-nuclei approximation.

Although the fractional charge nuclei do not directly represent realizable systems, they are useful in modeling the effect of the screening of nuclear charges in chemical bondings [9–13]. The profile of the energy curves of the present system was previously studied by Cohen and McEachran [9] and by Feinberg [10]. They reported the appearances of the potential barrier in the $1s\sigma_g$ ground state for $1 < Z < 1.44$ and the bonding energy minimum in the $2p\sigma_u$ state for $Z < 1$. The potential barrier in the $1s\sigma_g$ state has also been used as a model of the potential barrier observed for some diatomic molecular ions like He_2^{2+} [14].

In the following, we examine the Z effect on the interaction process from the viewpoint of force and density. Sect. 2 provides an outline of the concept of Berlin diagram and binding/antibinding analyses. In Sect. 3, the results are discussed in detail for the $1s\sigma_g$ and $2p\sigma_u$ states.

2. Theoretical Ground

The electron density in a diatomic system is spatially divided into the binding and antibinding parts by the Berlin diagram [1, 2]. Fig. 1 exemplifies this partitioning for the $1s\sigma_g$ state of H_2^+ system. Then the contribution of the electron density to a one-electron property G of the diatomic system is distinguished

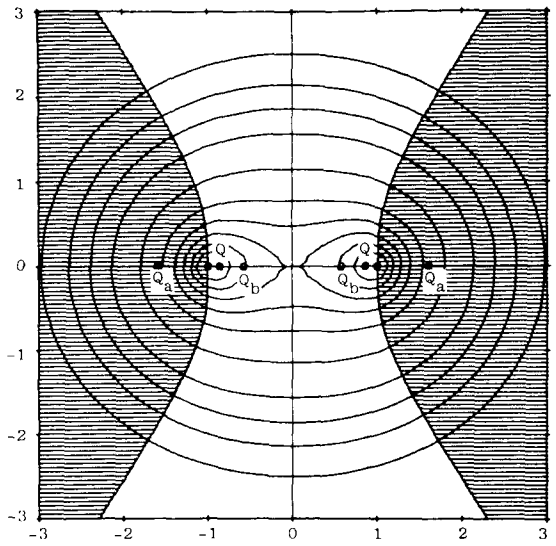

Fig. 1. Berlin diagram superposed on the $1s\sigma_g$ density distribution of the H_2^+ molecule ($R = 2$ a.u.). The antibinding regions are shaded. The positions of the total, binding, and antibinding CEDs are also shown. The contour values are 0.15, 0.125, 0.1, 0.075, 0.05, 0.025, 0.01, 0.005, 0.0025, and 0.001 a.u. from the innermost line

between the binding G_b and antibinding G_a contributions by the regional integration. (Hereafter, subscripts b, a, e, and n mean binding, antibinding, electronic, and nuclear contributions, respectively.)

In this study, we apply the binding-antibinding partitioning to the electronic charge N ($=N_b+N_a$), Hellmann–Feynman force F ($=F_e+F_n$; $F_e=F_b+F_a$), and CED Q ($=(N_bQ_b+N_aQ_a)/N$), and by pursuing the behaviours of these physical quantities, we investigate the change in the nature of interaction caused by the change of nuclear charge Z. (See Appendix and Ref. [6] for the definitions of the quantities F and Q.) For the energy extrema, stabilization energy ΔE and quadratic force constant k_e are also examined which are respectively obtained by integrating and differentiating the force F with respect to the internuclear distance R.

Using the electron density obtained from the exact wave function [15–18], we have first performed the calculation of the partitioned physical quantities for the bonding $1s\sigma_g$ and antibonding $2p\sigma_u$ states of the H_2^+ system ($Z=1$) as a function of R. The corresponding quantities for the nuclear charge other than unity are succeedingly obtained by utilizing the scaling relations valid in the one-electron homonuclear system. For example, N_b, F, and Q satisfy the following relations.

$$N_b(Z,R)=N_b(1,ZR),$$

$$F(Z,R)=Z^3\{F_e(1,ZR)+ZF_n(1,ZR)\},$$

$$Q(Z,R)=Z^{-1}Q(1,ZR).$$

Further details of the scaling relations are shown in Appendix.

The change of the nuclear charge Z is expected to have two opposite effects on the density reorganization during the interaction processes. When Z increases, one is an increase of the localization of the electron density in the neighbourhood of the nuclei (Effect (1)). This gives rise to decreases in the binding charge and the inward shift of CED, corresponding to a decrease of the electron density preceding (or an increase of the electron density following) [20]. This effect may work to increase the repulsion in cooperation with the nuclear force. The other is an increase of the attractive force due to the adjacent nucleus acting on the electron density (Effect (2)). The transfer of the density into the internuclear binding region is accelerated by this effect. Consequently, the binding charge and the inward shift of CED increase, corresponding to an increase of the electron density preceding (or a decrease of the electron density following) [20]. Effect (2) may contribute to increase the attractive force against Effect (1). When Z decreases, these effects work in a reverse direction. It is expected that at a large R, Effect (1) is predominant, while at a small R, Effects (1) and (2) are comparable. These expectations are examined quantitatively in the next section.

3. Effect of Nuclear Charge

3.1. Bonding $1s\sigma_g$ State

For several Z, the Hellmann–Feynman force and its components are shown in Fig. 2 as a function of R. As R decreases, the total force (Fig. 2a) for $Z = 1$ (H_2^+ system) monotonically increases its attraction with the minimum (-0.0342 a.u.) at $R = 2.99$ a.u. Then the force becomes repulsive passing through

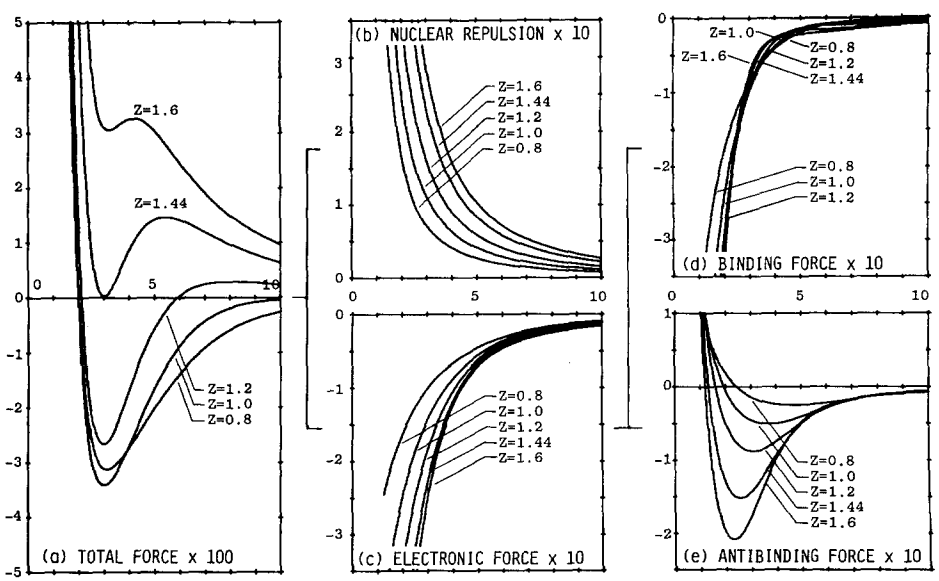

Fig. 2. The $1s\sigma_g$ state. Binding-antibinding partitioning of the Hellmann–Feynman force. Negative and positive values mean attractive and repulsive contributions, respectively

the equilibrium distance R_e ($=2.00$ a.u.) where the force vanishes. For $Z<1$, the total force behaves similarly to that of H_2^+, though the relative magnitudes of attraction are different in the initial and intermediate stages (see the curve for $Z=0.8$).

For $1<Z<1.44$, however, the total force shows initial repulsion and the succeeding change into attraction (see $Z=1.2$). This implies the existence of potential barrier whose peak is located at the critical distance R_e^* of zero force. (The asterisk means the property of potential barrier.) The appearance of repulsive force for $Z>1$ is expected from the long-range perturbation theory, since the leading term of long-range force for the present system consists of the electronic part $-Z/R^2$ and the nuclear part $+Z^2/R^2$ [21]. In the final stage, the total force again changes into repulsion and the stable equilibrium is also observed in this Z range. At $Z=1.44$, the force curve contacts with the abscissa of $F=0$ and R_e coincides with R_e^*. This corresponds to a terrace of the stabilization energy curve. For $Z>1.44$, the force is repulsive throughout the whole range of R and no stable molecule is formed.

The properties of the potential barrier appearing in the $1s\sigma_g$ state are summarized in Table 1 for several Z. With the increase of Z, k_e^* decreases and ΔE^* increases reflecting the increase of instability. The region of repulsive force also increases and R_e^* lowers. The corresponding properties of the stable equilibrium are shown in Table 2. Though R_e takes its minimum at $Z\sim0.79$, it suffers rather small Z effect than expected (see also Fig. 2a). The quadratic force constant k_e is maximum at $Z\sim1.03$, while the stabilization energy ΔE is minimum at $Z\sim0.74$. The neutral system ($Z=0.5$) is not the most stable system. For $Z>1.24$, ΔE is positive and the system is less stable than the separated atoms (SA).

Figs. 2b and c show the partitioning of the total force into the electronic and nuclear parts. Though the electronic attraction and the nuclear repulsion increase monotonically with increasing Z and decreasing R, the Z effect is larger for the nuclear part in the initial stage and for the electronic part in the intermediate stage. The total force is seen to be a result of subtle balance of these opposing forces. In Figs. 2d and e, the electronic force (Fig. 2c) is further decomposed

Table 1. Properties of potential barrier in the $1s\sigma_g$ state. Potential barrier appears for $1<Z<1.4391$

Z	R_e^*/a.u.	k_e^*/a.u.	ΔE^*/a.u.
1[a]	∞	0	0
1.1	7.676	−0.0012	0.01212
1.2	5.938	−0.0039	0.03311
1.3	4.752	−0.0083	0.06435
1.4	3.710	−0.0112	0.10905
1.4391[b]	3.009	0	0.13180

[a] Normal H_2^+ molecule.
[b] Two potential extrema coalesce at this Z value.

Table 2. Properties of stable H_2^+ analogues in the $1s\sigma_g$ state as a function of Z

Z	R_e/a.u.	k_e/a.u.	ΔE/a.u.
0[a]	∞	0	0
0.1	3.882	0.0003	−0.01051
0.2	2.813	0.0031	−0.03358
0.3	2.402	0.0101	−0.06146
0.4	2.189	0.0214	−0.08915
0.5	2.067	0.0364	−0.11303
0.6	1.998	0.0533	−0.13043
0.7	1.962	0.0703	−0.13934
0.8	1.952	0.0855	−0.13829
0.9	1.964	0.0970	−0.12627
1[b]	1.997	0.1030	−0.10263
1.1	2.053	0.1017	−0.06717
1.2	2.140	0.0918	−0.02006
1.3	2.279	0.0705	+0.03789
1.4	2.558	0.0326	0.10466
1.4391[c]	3.009	0	0.13180

[a] Limit of free electron.
[b] Normal H_2^+ molecule.
[c] Two potential extrema coalesce at this Z value.

into the binding and antibinding parts based on the Berlin diagram (Fig. 1). (The net changes from the SA values are plotted in these figures.) As R decreases, the binding force monotonically increases its attraction and the Z effect is found to be small (Fig. 2d). On the other hand, the antibinding force decreases its repulsion (i.e. attractive contribution) with decreasing R and shows a large dependence on Z (Fig. 2e). The increase of Z contributes to increase the attraction and this is quite remarkable in the intermediate stage. The behaviour of the antibinding force resembles that of the total force for $Z < 1.44$ and the antibinding part is seen to give a significant contribution to the attractive nature of the Hellmann–Feynman force. Consequently, the initial repulsion and the succeeding attraction of the system for $1 < Z < 1.44$ are attributed respectively to the increased nuclear repulsion and to the decreased antibinding force. Feinberg [10] also pointed out that the nuclear part is responsible for the appearance of potential barrier from the energetic point of view.

Next, we investigate the reorganization of electron density which governs the forces discussed above. The changes of the binding charge and CED and its components during the interaction process are shown in Figs. 3a–d. The binding charge increases as R decreases and takes maximum value ($0.724e^-$) at $R =$ 1–3 a.u. (Fig. 3a). As understood from the scaling relation (see Appendix), the maximum value is independent of Z. The total CED shifts towards the center of bond except for a small R (Fig. 3b).

The behaviour of the binding charge and the total CED shows that the Z effect on the electron density in the initial and intermediate stages belongs to Effect

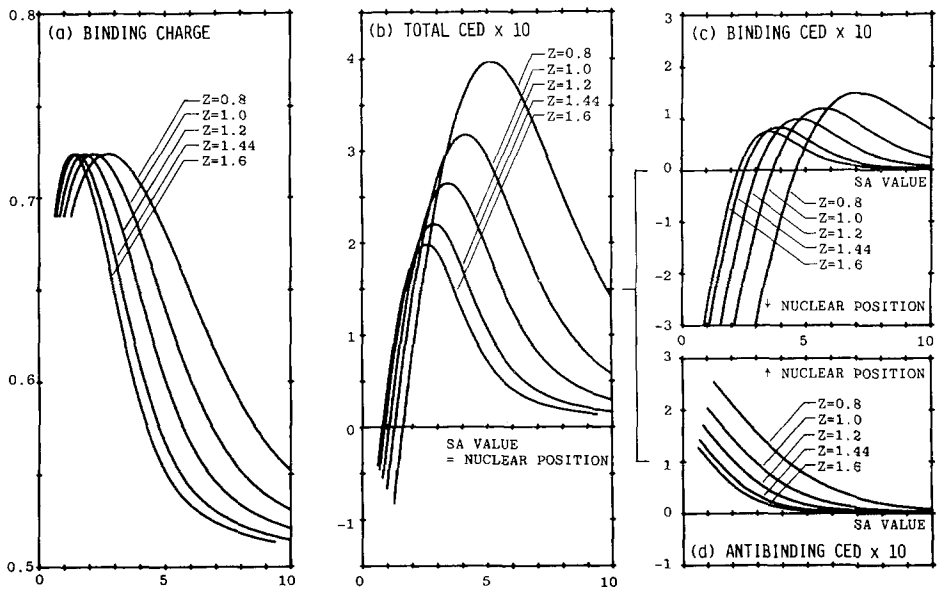

Fig. 3. The $1s\sigma_g$ state. (a) Binding charge. The SA value is $0.5e^-$. (b–d) CED and its binding-antibinding components. The corresponding SA values have been subtracted. Therefore, positive values mean the shifts of CEDs towards the center of bond, while negative values mean the shifts towards the outside

(1) mentioned in Sect. 2. Namely, the increase of Z accelerates the localization of density around the nuclei leading to the decrease in the binding charge and the inward shift of CED. This is a decrease of the density preceding and works to reduce the attractive contribution of the electronic force. The same trend has been observed in the repulsive ground state of the HeH^{2+} system [7]. For $R = 1$–3 a.u. however, Effect (2) becomes dominant and promotes the delocalization of density into the internuclear region. In this R range, the increase of Z results in the increase of the binding charge and the inward shift of CED. This is an increase of density preceding.

The binding CED (Fig. 3c) which represents the centroid of binding density decreases in the initial and intermediate stages as Z increases (Effect (1)). This density reorganization works to reduce the binding force. However, the force operator itself is proportional to Z, and hence the binding force remains almost unchanged. When Z decreases from unity, the situation is opposite and again results in small Z dependence of the binding force (Fig. 2d). In the final stage, however, Effect (2) becomes predominant and the binding force is in proportion to Z (see e.g. $R = 2$ a.u. in Fig. 2d).

On the other hand, the antibinding CED shows a monotonic shift towards the nuclei throughout the process (Fig. 3d). The shift is small for large Z, corresponding to a small increase in the binding charge. Therefore, the antibinding density is more localized near the nuclei than the binding density irrespective of Z. A

decrease in this localized antibinding density is the origin of large attractive contribution of the antibinding force (Fig. 2e). The results again support the previous suggestion [6] that of the two regional density reorganizations, the decrease in the localized antibinding density is more effective to the binding and stabilization of the system than the increase in the delocalized binding density, though they occur simultaneously and are cooperative. Figs. 2d and e further suggest that this tendency becomes larger as Z increases.

3.2. *Antibonding* $2p\sigma_u$ *State*

The results of the binding/antibinding analyses for the $2p\sigma_u$ state are given in Figs. 4 and 5.

As seen in Fig. 4a, the total force is repulsive for $Z \geq 1$ and no stable molecule is formed. The increase in Z merely increases the repulsion of the system (see $Z = 1.2$ in Fig. 4a). For $Z < 1$, however, attractive force appears in a large R range (curves for $Z = 0.6$ and 0.8). The attraction is maximum at $R = 10$–15 a.u. and then the force changes into repulsion. This behaviour of the total force means that for $Z < 1$ a stable molecule can be formed even in the "antibonding" $2p\sigma_u$ state. The properties of this equilibrium are summarized in Table 3. All the R_e, k_e, and ΔE suggest the most stable system at $Z = 0.6$–0.8, though the stability is only about a sixth of that of the $1s\sigma_g$ state.

To investigate the origin of this unexpected attraction in the $2p\sigma_u$ state, we have decomposed the total force into the components in Figs. 4b–e. The electronic and nuclear parts show similar Z dependences and the origin of attraction is not clear at this level of partitioning. When the electronic force is further

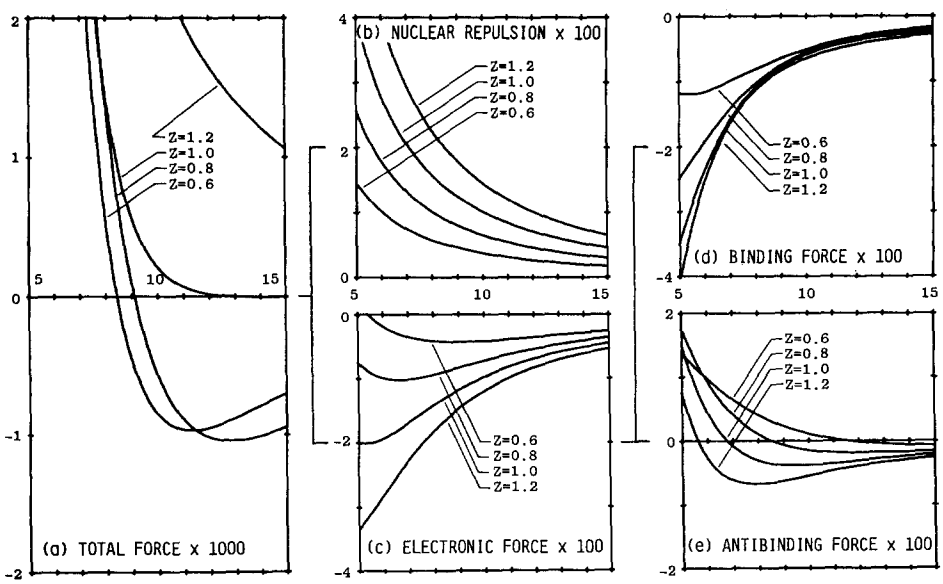

Fig. 4. The $2p\sigma_u$ state. See the captions to Fig. 2

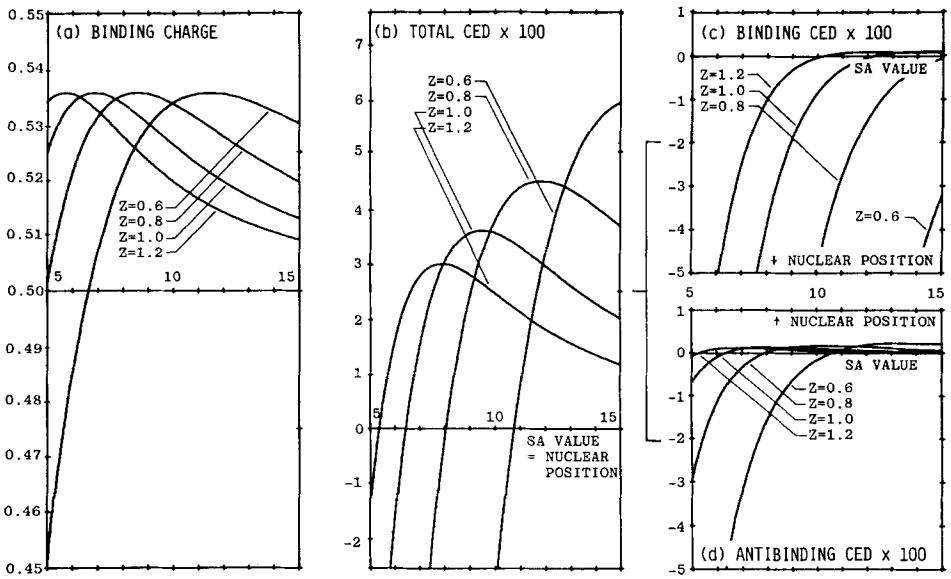

Fig. 5. The $2p\sigma_u$ state. See the captions to Fig. 3

partitioned, the binding force (Fig. 4d) is found to slightly decrease its attraction with the decrease of Z. However, the Z dependence is very small for $R > 10$ a.u. (Note the variance between the scales of Figs. 2 and 4.) The antibinding force (Fig. 4e) also contributes to the attraction for a large R. As Z decreases, the attraction decreases and terminates at a larger R. The extent of the Z effect is larger than that for the binding force, and is comparable to that for the electronic force. The decrease of the nuclear repulsion due to the decrease in Z is nearly cancelled with the increase of the antibinding force. Thus the attraction appearing

Table 3. Properties of potential minimum in the $2p\sigma_u$ state. Potential minimum appears for $Z < 1$

Z	R_e/a.u.	$k_e \times 100$/a.u.	$\Delta E \times 10$/a.u.
0[a]	∞	0	0
0.1	35.47	0.0002	−0.01727
0.2	19.38	0.0032	−0.05828
0.3	14.06	0.0129	−0.10887
0.4	11.46	0.0317	−0.15713
0.5	9.983	0.0580	−0.19323
0.6	9.096	0.0861	−0.20922
0.7	8.598	0.1055	−0.19916
0.8	8.437	0.1041	−0.15946
0.9	8.750	0.0692	−0.09002
1[b]	∞	0	0

[a] Limit of free electron.
[b] Normal H_2^+ molecule.

for $Z < 1$ may be attributed to the binding force which has small Z dependence. The smaller Z effect on the binding force is common to the $1s\sigma_g$ and $2p\sigma_u$ states.

The density origin of the Hellmann–Feynman force is shown in Fig. 5. The binding charge (Fig. 5a) slightly increases with the decrease of R. Though the maximum value (0.537e^-) is larger than the SA value (0.5e^-), it is considerably smaller than that of the bonding state (0.724e^-). With the decrease of Z, the binding charge increases for a large R and decreases for a small R. This is Effect (1) for the loosely-bound density due to a smaller Z. Correspondingly, the total CED shows inward shift whose degree is larger for smaller Z. These imply the presence of small density preceding in the antibonding state. In this R range, the component CEDs show a large localization of the binding density towards the nuclei (Fig. 5c) and an almost-unchanged distribution of the antibinding density (Fig. 5d). As in the $1s\sigma_g$ state, these reorganization of the regional densities result in small and large Z dependences of the binding and antibinding forces, respectively, through Z in the force operator. For a small R, however, the nodal property of the $2p\sigma_u$ state is dominant and the decreases of the binding charge and CEDs, which contribute to the repulsion of the system, are remarkable. For respective values of Z, the inward/outward shifts of the antibinding CED (Fig. 5d) well correspond to the attractive/repulsive contributions of the antibinding force (Fig. 4e).

The present results of the binding/antibinding analyses show that the effect of nuclear charge is larger for the binding density than for the antibinding density commonly to the $1s\sigma_g$ and $2p\sigma_u$ states. Then the density reorganization in the binding region, which may characterize the nature of chemical bonding, is suggested to be very sensitive to the "effective" nuclear charge resulting from the shielding by core electrons and so on. However, the Z effect on the binding density is cancelled with Z in the force operator, and therefore the antibinding part reveals a significant Z dependence in the interatomic force. This is also true for the partitioned stabilization energies when the forces are integrated. We must distinguish between the Z dependence of density reorganization and that of interatomic force and stabilization energy.

4. Summary

In this study, we have quantitatively examined the effect of nuclear charge on one-electron diatomic interactions from the force and density point of view.

For both the $1s\sigma_g$ and $2p\sigma_u$ states, the Z effect is larger for the binding density than for the antibinding density. However, the dominancy is interchanged for the partitioned forces, since the force operator is proportional to Z.

In the $1s\sigma_g$ state, the increase in Z causes two energy extrema (configurations with zero force) for $1 < Z < 1.44$. One is potential barrier in the initial stage of the interaction which is attributed to the dominance of the nuclear repulsion in this R range. The other is potential minimum at a shorter R which results from the decrease of the antibinding force. As in a previous study [6], the reorganiz-

ation of the localized antibinding density is found to be more important than that of the delocalized binding density even when Z is varied.

In the "antibonding" $2p\sigma_u$ state, the bonding nature emerges and a stable molecule is formed for $Z < 1$. The decrease of Z reduces the attractive contribution of the antibinding force, and hence the binding force with small Z dependence is responsible for the weak attraction in this state.

Acknowledgment. Part of this study has been supported by a Grant-in-Aid for Scientific Research from the Ministry of Education of Japan.

Appendix. Scaling Relations for One-Electron Homonuclear Systems

The most fundamental relation is

$$\rho(r; Z, R) = Z^3 \rho(Zr; 1, ZR)$$

for the electron density, which immediately follows from the scaling relation for the one-electron wave function $\Psi(r; Z, R) = Z^{3/2}\Psi(Zr; 1, ZR)$.

(1) Hellmann–Feynman Force
For the electronic part, the force operator satisfies

$$\begin{aligned} f(r; Z, R) &= (1/2)(Z \cos\theta_A / r_A^2 + Z \cos\theta_{A'} / r_{A'}^2) \\ &= Z^3 f(Zr; 1, ZR). \end{aligned}$$

Then the scaling relation for the binding force is

$$\begin{aligned} F_b(Z, R) &= -\int_{f(r;Z,R)>0} f(r; Z, R)\rho(r; Z, R)\, dr \\ &= -Z^3 \int_{f(Zr;1,ZR)>0} f(Zr; 1, ZR)\rho(Zr; 1, ZR)\, d(Zr) \\ &= Z^3 F_b(1, ZR). \end{aligned}$$

Similarly $F_a(Z, R) = Z^3 F_a(1, ZR)$ and the sum of the two relations yields the relation for the electronic force

$$F_e(Z, R) = Z^3 F_e(1, ZR).$$

Since the nuclear part is simply

$$F_n(Z, R) = Z^2/R^2 = Z^4 F_n(1, ZR),$$

the scaling relation for the total force is found to be

$$\begin{aligned} F(Z, R) &= Z^3\{F_e(1, ZR) + ZF_n(1, ZR)\} \\ &= Z^3\{F(1, ZR) + (Z-1)/(ZR)^2\}. \end{aligned}$$

(2) Electronic Charge
For the binding charge, we get

$$\begin{aligned} N_b(Z,R) &= \int_{f(r;Z,R)>0} \rho(r;Z,R)\,dr \\ &= \int_{f(Zr;1,ZR)>0} \rho(Zr;1,ZR)\,d(Zr) \\ &= N_b(1,ZR). \end{aligned}$$

Similarly, $N_a(Z,R)=N_a(1,ZR)$ for the antibinding charge. The total charge $N=N_b+N_a$ is conserved irrespective of Z and R (unity in the present case).

(3) CED (Center of Electron Density)
The binding CED satisfies

$$\begin{aligned} Q_b(Z,R) &= \int_{Ab} r\rho(r;Z,R)\,dr \Big/ \int_{Ab} \rho(r;Z,R)\,dr \\ &= Z^{-1} \int_{Ab} (Zr)\rho(Zr;1,ZR)d(Zr) \Big/ \int_{Ab} \rho(Zr;1,ZR)\,d(Zr) \\ &= Z^{-1}Q_b(1,ZR), \end{aligned}$$

where $\int_{Ab} dr$ denotes the integration over the atomic binding region [6]. Similarly, $Q_a(Z,R)=Z^{-1}Q_a(1,ZR)$ for the antibinding CED, and for the total CED, $Q(Z,R)=Z^{-1}Q(1,ZR)$, from $Q=(N_bQ_b+N_aQ_a)/N$.

(4) Stabilization Energy
The scaling relation for ΔE is obtained by integrating F with respect to R. For example, the binding contribution satisfies

$$\begin{aligned} \Delta E_b(Z,R) &= \int_{\infty}^{R} [F_b(Z,R')-F_b(Z,\infty)]\,dR' \\ &= Z^2 \int_{\infty}^{ZR} [F_b(1,ZR')-F_b(1,\infty)]\,d(ZR') \\ &= Z^2 \Delta E_b(1,ZR). \end{aligned}$$

Similarly, we get $\Delta E_a(Z,R)=Z^2\Delta E_a(1,ZR)$, $\Delta E_e(Z,R)=Z^2\Delta E_e(1,ZR)$, and $\Delta E_n(Z,R)=Z^3\Delta E_n(1,ZR)$ for the antibinding, electronic, and nuclear contributions. The sum gives

$$\begin{aligned} \Delta E(Z,R) &= Z^2\{\Delta E_e(1,ZR)+Z\Delta E_n(1,ZR)\} \\ &= Z^2\{\Delta E(1,ZR)+(Z-1)/(ZR)\}, \end{aligned}$$

which agrees with the known result [13, 19].

(5) Force Constant

We define $k(Z,R) = -dF(Z,R)/dR$. Then the force constant $k_e(Z) = k(Z,R)|_{R=R_e(Z)}$ satisfies

$$\begin{aligned} k_e(Z) &= -dF(Z,R)/dR|_{R=R_e(Z)} \\ &= Z^4\{-dF(1,ZR)/d(ZR) + 2(Z-1)/(ZR)^3\}|_{R=R_e(Z)} \\ &= Z^4 k(1,ZR)|_{R=R_e(Z)} + 2Z(Z-1)/(R_e(Z))^3. \end{aligned}$$

The same result also follows from the second derivative of ΔE.

References

1. Berlin, T.: J. Chem. Phys. **19**, 208 (1951)
2. Koga, T., Nakatsuji, H., Yonezawa, T.: J. Am. Chem. Soc. **100**, 7522 (1978)
3. Hellmann, H.: Einführung in die Quantenchemie, Vienna: Deuticke 1937; Feynman, R. P.: Phys. Rev. **56**, 340 (1939)
4. Deb, B. M.: Rev. Mod. Phys. **45**, 22 (1973); Bamzai, A. S., Deb, B. M.: Rev. Mod. Phys. **53**, 95 (1981)
5. Deb, B. M., ed.: The force concept in chemistry, New York: Van Nostrand Reinhold 1981
6. Koga, T., Nishijima, T., Morita, M.: Theoret. Chim. Acta (Berl.) **55**, 133 (1980)
7. Koga, T., Morita, M.: Theoret. Chim. Acta (Berl.) **56**, 113 (1980)
8. Koga, T., Morita, M.: Chem. Phys. **54**, 387 (1981)
9. Cohen, M., McEachran, R. P.: Theoret. Chim. Acta (Berl.) **12**, 87 (1968)
10. Feinberg, M. J.: Theoret. Chim. Acta (Berl.) **19**, 109 (1970); Feinberg, M. J., Ruedenberg, K.: J. Chem. Phys. **55**, 5804 (1971)
11. Dunitz, J. D., Ha, T. K.: J. Chem. Soc. Chem. Commun. 568 (1972)
12. Tal, Y., Katriel, J.: Mol. Phys. **30**, 621 (1975); Merksamer, R., Katriel, J.: Chem. Phys. Lett. **52**, 171 (1977)
13. Laurenzi, B. J.: Theoret. Chim. Acta (Berl.) **13**, 106 (1969); J. Chem. Phys. **65**, 217 (1976); **74**, 1840 (1981)
14. Pauling, L.: J. Chem. Phys. **1**, 56 (1933); Fraga, S., Ransil, B. J.: J. Chem. Phys. **37**, 1112 (1962); Feinberg, M. J., Haas, T. E.: Theoret. Chim. Acta (Berl.) **7**, 290 (1967)
15. Bates, D. R., Ledsham, K., Stewart, A. L.: Phil. Trans. R. Soc. London, **A246**, 215 (1954); Bates, D. R., Reid, R. H. G.: Adv. At. Mol. Phys. **4**, 13 (1968)
16. Wallis, R. F., Hulbert, H. M.: J. Chem. Phys. **22**, 774 (1954)
17. Peek, J. M.: J. Chem. Phys. **43**, 3004 (1965); Madsen, M. M., Peek, J. M.: At. Data **2**, 171 (1971)
18. Teller, E., Sahlin, H. L., in: Physical chemistry. Vol. 5, Valency, Eyring, H., (ed.). New York: Academic 1970
19. Cohen, M., Dorrell, B. H., McEachran, R. P.: Theoret. Chim. Acta (Berl.) **9**, 324 (1968); Davidson, E. R., in: Physical chemistry, Vol. 3, Electronic structure of atoms and molecules, Henderson, D., (ed.). New York: Academic 1969
20. Nakatsuji, H.: J. Am. Chem. Soc. **95**, 2084 (1973); **96**, 24, 30 (1974); Nakatsuji, H., Koga, T.: Chapter 3 of Ref. 5
21. Coulson, C. A.: Proc. Roy. Soc. Edinburgh, **A61**, 20 (1941); Nakatsuji, H., Koga, T.: J. Am. Chem. Soc. **96**, 6000 (1974)

Received May 25, 1982